Observation of Photochemical C−N Bond Cleavage in CH_3N_3: A New Photochemical Route to Cyclic N_3

Christopher Larson,*,† Yuanyuan Ji,† Peter C. Samartzis,† Alfredo Quinto-Hernandez,† Jim Jr-Min Lin,‡ Tao-Tsung Ching,§ Chanchal Chaudhuri,§ Shih-Huang Lee,§ and Alec M. Wodtke†

Department of Chemistry and Biochemistry, University of California, Santa Barbara, Santa Barbara, California 93106-9510, Institute of Atomic and Molecular Sciences, Academia Sinica, P.O. Box 23-166, Taipei 106, Taiwan, Republic of China, and National Synchrotron Radiation Research Center, 101 Hsin-Ann Road, Hsinchu 30077, Taiwan, Republic of China

Received: August 23, 2007; In Final Form: December 6, 2007

We report VUV-photoionization based photofragmentation-translational spectroscopy data, providing a comprehensive study of the collision free photochemistry of methyl azide (CH_3N_3) at 193 nm. We report the first observation of the production of methyl and the N_3 radical and derive the translational energy release distribution of this reaction. The most probable translation energy is only 8%, and the maximum translational energy is only 60% of the available energy, taking CH_3 + linear N_3 as the zero of energy. However, the maximum translational energy release is quantitatively consistent with production of the higher energy isomer cyclic N_3. Threshold photoionization of the N_3 fragment using tunable synchrotron radiation shows results consistent with theoretical predictions of the cyclic N_3 ionization potential. The secondary dissociation of $N_3 \rightarrow N(^2D) + N_2$ is also observed and its translational energy release is derived. This distribution peaks at ∼6 and extends to 11 kcal/mol as would be expected from the size of the exit channel barrier for spin-allowed dissociation of cyclic N_3 (7 kcal/mol) and, furthermore, inconsistent with the barrier height of the spin-allowed dissociation of linear N_3 (3 kcal/mol). A large fraction (∼45%) of the N_3 does not dissociate on the microsecond time scale of the experiment suggesting methyl azide may be the most attractive photochemical precursor of cyclic N_3 yet found.

Introduction

Collision-free studies of azide photochemistry, which began only recently,[1−10] have provided some interesting surprises. Of the two possible primary photodissociation channels

$$XN_3 + h\nu \rightarrow X + N_3 \qquad \text{(radical channel)}$$

$$XN_3 + h\nu \rightarrow XN + N_2 \qquad \text{(molecular elimination)}$$

the radical channel has been found to be more important than previously suspected.[3,4] Furthermore, we now have compelling evidence, which has recently been reviewed,[1,2] that the N_3 radical formed by the simple bond rupture reaction may appear in two forms: the well-known linear azide and a theoretically predicted cyclic form.[3,5,6,11−13]

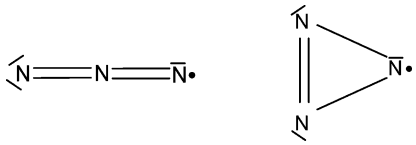

So far, the most informative and extensive experiments have been performed on ClN_3, where it has been found that as the photon energy, $h\nu$, is increased from ∼4.4 eV a threshold for cyclic N_3 formation is observed at $h\nu \sim 4.9$ eV;[5] cyclic N_3 production is significant at 5 eV[3,13] and dominant at 6.4[2,9] and 7.8 eV.[12] Recently, an accurate N−Cl bond energy has been reported, $D_0(Cl-N_3) = 1.86$ eV.[14] This points out one of the difficulties in efficiently producing cyclic N_3 from ClN_3, since under conditions where cyclic N_3 is produced efficiently the majority of the molecules are produced with so much internal energy that they undergo subsequent unimolecular decomposition even under collision free conditions. Thus, it is worth considering other azides where the electronic structure might be similar, but where the $X-N_3$ bond is stronger and where X might also be a polyatomic capable of carrying away more energy in its internal degrees of freedom.

Within this context, methyl azide, CH_3N_3, is a reasonable candidate with a C−N bond-energy of ∼3.2 eV (nearly twice $D_0(Cl-N_3)$) and an electronic absorption spectrum similar to FN_3.[15,16] This suggests that UV photodissociation in the photon-energy range of 5−8 eV might be an improved way to produce cyclic N_3. We have previously reported the collision free photochemistry of CH_3N_3 at 248-nm ($h\nu = 4.99$ eV).[10] In that work despite extensive attempts, no evidence of the radical channel mentioned above could be found; however, we observed the molecular elimination channel and subsequent unimolecular decomposition of methylnitrene, leading to HCN and HNC by different pathways.

$$H_3C-N-N\equiv N \rightarrow H_3C-N + N_2 \qquad \text{(R1, molecular elimination)}$$

$$H_3C-N \rightarrow H_2C{=}NH \qquad \text{(methylnitrene isomerization)}$$

* To whom correspondence should be addressed. E-mail: clarson@chem.ucsb.edu. Tel: (805) 893-5035. Fax: (805) 893-4120.
† University of California, Santa Barbara.
‡ Academia Sinica.
§ National Synchrotron Radiation Research Center.

10.1021/jp076779h CCC: $40.75
Published on Web 01/23/2008

$H_2C{=}NH \rightarrow H_2C{=}N + H$ (HCN formation step 1)

$H_2C{=}N \rightarrow HC{\equiv}N + H$ (HCN formation step 2)

$H_2C{=}N{-}H \rightarrow H_2 + C{\equiv}N{-}H$ (HNC formation)

In contrast, this work at a substantially shorter photolysis wavelength (λ = 193-nm; $h\nu$ = 6.41 eV) reveals similar molecular elimination photochemistry as well as the first observation of the simple bond rupture reaction (R2)

$$CH_3N_3 + h\nu \rightarrow CH_3 + N_3 \quad \text{(R2)}$$

Using near-threshold VUV-photoionization based photofragmentation translational spectroscopy; we derive the translational energy release distribution of reaction (R2) and find that it is consistent with the exclusive formation of cyclic N_3. We also observe and analyze the secondary dissociation of the N_3 photofragment and derive its translational energy release distribution. The translational energy release of this reaction is remarkably large, peaking at 5-kcal/mol and extending to the energetic limit of 10-kcal/mol. This is additional and uniquely compelling evidence for the formation of cyclic N_3 as the theoretically predicted exit barrier for cyclic N_3 dissociation is much larger (7 kcal/mol) than that of linear N_3 (3 kcal/mol). We also report photoionization yield vs photoionization energy for the N_3 photofragment, which reveals an ionization threshold similar to theoretical predictions[17,18] and experimental reports of cyclic N_3.[13] Validating the logic outlined above, we do indeed find that a large fraction (~45%) of the initially formed cyclic N_3 survives to the detector after a $\sim 10^{-4}$ s flight time. Similar survival fractions for cyclic-N_{-3} formed in ClN_3 photolysis are all smaller.[2,3,5,9,12,13] In particular due to the large fraction of surviving N_3, methyl azide would appear to be an attractive candidate for efficient cyclic N_3 production.

Experimental Methods

The experiments described here are quite similar to previous reports,[10,19] and only essential experimental conditions are presented. Methyl azide was synthesized by reacting sodium azide with methyl iodide in a 4:1 DMF/water solution analogous to previously reported chemistry.[20] The product was analyzed by NMR,[21] which showed methyl azide and a small amount of methyl iodide contaminant. The sample was used without further purification. The experiments were carried out at the Chemical Dynamics Beamline 21A at the National Synchrotron Radiation Research Center in Hsinchu, Taiwan. Liquid methyl azide samples were placed in a glass bubbler and kept at −15 °C (vapor pressure of ~150 Torr). Helium carrier gas was passed through the liquid, and the total backing pressure entering the source chamber was ~270 Torr. A molecular beam was generated by a solenoid-driven pulsed valve (General Valve), and the beam was intersected at 90° by an unpolarized, focused (8 mm by 3.5 mm with laser spot size narrower in the direction of the detector) 193 nm ArF excimer laser beam. The photofragmentation machine uses a rotating source chamber with a fixed detector.[19] With the source-detector angle placed at either $\Theta_L = 30°$ or 60°, the resulting neutral photofragments flew over a 10.05 cm distance where they were intersected at right angles by a focused beam of synchrotron radiation, ionized, and mass selected by a quadrupole mass filter (QMF) before reaching a Daly style detector for ion counting. Most data were averaged over 20 000−80 000 laser shots. Experiments could be carried out at various photoionization energies ($h\nu_{\text{photoionization}}$) by changing the gap of the beam line Undulator. Experiments reported here were performed at $h\nu_{\text{photoionization}}$ = 15.9, 13.3, 12.83, and 11.9 eV. The resolution of the ionizing radiation was about 3% or ±0.15 eV. Mass-resolved, time-of-flight (TOF) spectra were obtained at mass-to-charge (m/z) ratios of 14, 15, 27, 28, 29, and 42 amu.

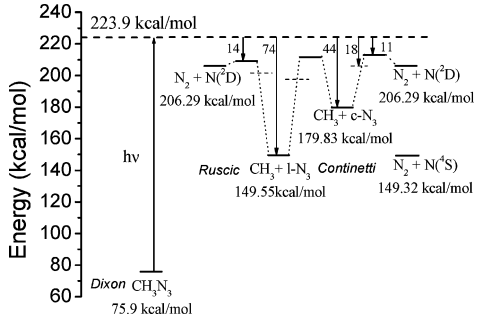

Figure 1. Energetic diagram for primary and secondary dissociation processes for the radical channel (C−N rupture) of methyl azide dissociation. The zero-Kelvin heats of formation are indicated with references to primary literature. "*hν*" indicates a single 193-nm photon (148 kcal/mol). The energetics of ring closing of N_3 and the barrier height for dissociation of linear and cyclic N_3 are taken from refs 11 and 28. The dashed lines indicate the position where calculated quartet seam crossing minima have been identified.

Data obtained in this experiment was analyzed using the highly accurate forward convolution fitting approach. Two computer programs were required in order to model both primary and secondary dissociation processes. Parameters which accurately describe the experimental conditions are input into PHOTRAN[22] which then simulates a TOF spectrum based on a user input translational energy probability distribution, $P(E_T)$. The input experimental parameters include: molecular beam velocity and angular distribution, detector flight length, sizes of laser and ionization volumes, detector angular acceptance width and several other instrumental factors. The $P(E_T)$ is adjusted until the simulated spectrum matches the experimental data. PHOTRAN, however, is only capable of modeling primary dissociation. For secondary dissociation analysis, the computer program ANALMAX[23] was used. ANALMAX also accepts a wide variety of information on all aspects of the experiment and then performs a brute-force forward convolution calculation. For both the primary and secondary dissociation, we used an anisotropy parameter $\beta = 0$, corresponding to an isotropic distribution.

Results and Analysis

A. C−N Bond-Rupture 'Radical' Channel. The results of this experiment are far easier to present within the context of an accurate energetic diagram of the available reaction channels. This is shown in Figure 1, which has been constructed from literature thermodynamics. Critical to our diagram is the heat of formation of methyl azide $\Delta_f H^{0K}(CH_3N_3)$ Apparently improving on earlier work, Gutowski et al. reported ab initio electronic structure calculations using an approach based on CCSD(T) extrapolation to the complete basis set (CBS) limit to predict heats of formation.[24] Based on a favorable comparison to experiment for the case of HN_3, the authors believe the uncertainty in the heat of formation of methyl azide, $\Delta_f H^{0K}(CH_3N_3)$, is less than 1 kcal/mol. For our analysis, we rely on this work for the $\Delta_f H^{0K}(CH_3N_3) = 75.9 \pm 1$ kcal/mol. We refer to Ruscic et al., who have critically reviewed thermochemical data on a number of free radicals, for the $\Delta_f H^{0K}(CH_3) = 35.85 \pm 0.07$ kcal/mol[25] and the work of Continetti et al. for the $\Delta_f H^{0K}$(linear N_3) = 113.7 ± 2

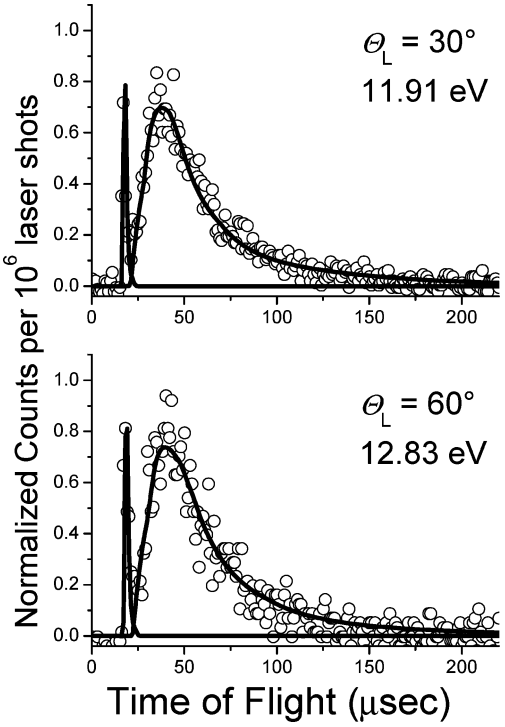

Figure 2. Representative TOF spectra for $m/z = 15$ (CH_3^+) arising from CH_3N_3 photolysis at 193 nm. The points are observed data rebinned to 1 μs channels and the solid line is the results of the forward convolution fitting analysis described in the text. The photoionization energy used for each TOF spectra is labeled. The sharp, early feature at ~20 μs arises from CH_3I impurity and has been fit separately, based on energy release data from Continetti et al.[29] The data has been normalized to laser power and the synchrotron radiation intensity.

kcal/mol.[26,27] From this we can derive the energy available to the products of reaction (R2 − radical channel), $E_{ava} = 74 \pm 3$ kcal/mol. In the case of production of cyclic N_3, an additional 30.3 ± 2 kcal/mol is lost to the potential energy associated with ring formation[28] leading us to the available energy to cyclic N_3 + CH_3 products: $E_{ava}^{cyc} = 44 \pm 5$ kcal/mol. Alternatively we may use a recently reported experimental determination of $\Delta_f H^{0K}$(cyclic N_3) =142 ± 3.5 to arrive at a value for $E_{ava}^{cyc} = 46 \pm 5$ kcal/mol.[12] As will be shown below, both of these results are closely consistent with the observed maximum translational energy release, $E_T^{max} = 45 \pm 4$ kcal/mol, seen in this work. We now turn to a description of the observed TOF spectra in this work.

Figure 2 shows TOF spectra obtained when the QMF is adjusted to pass $m/z = 15$ (CH_3^+). One can immediately discern that the TOF is made up of two contributions, a sharp early feature at about 20 μs and a later broader feature. The method of synthesis described in the experimental section produces a sample with a small CH_3I impurity and we will show that this impurity gives rise to the sharp, fast peak in the TOF spectra of Figure 2. To demonstrate this, we reanalyzed the 193-nm photofragmentation translational spectroscopy data of Continetti et al.[29] using the PHOTRAN program.[22] In that work, a neat beam of CH_3I was formed, and photofragment-TOF spectra were recorded with an instrument similar to the one used in this work. The fitting of that data provided a center-of-mass (COM) translational energy distribution, $P_{CH3I}(E_T)$, for the methyl-iodide photolysis that could be applied to the $m/z = 15$ TOF spectra obtained in this work. The use of $P_{CH3I}(E_T)$ leads to an excellent fit of the sharp fast feature of the TOF spectra shown in Figure 2. It is worth noting that the CH_3 from CH_3I is temporally well-resolved from the azide photoproduct. Thus, the impurity has little influence on the interpretation of our results.

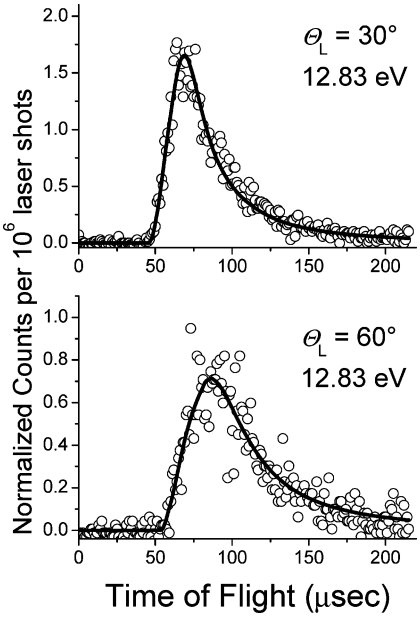

Figure 3. Representative TOF spectra for $m/z = 42$ (N_3^+) arising from CH_3N_3 photolysis at 193 nm. See caption of Figure 2 for further details.

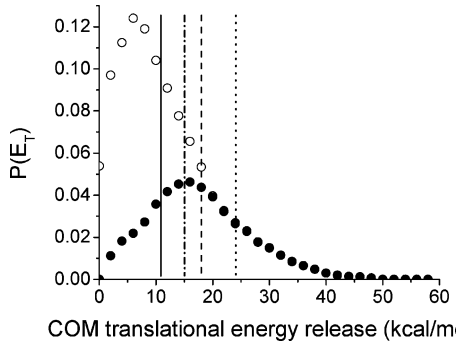

Figure 4. $P(E_T)$'s for C−N bond cleavage. Solid circles are derived from the $m/z = 42$ data, and open circles are from the $m/z = 15$ data. The difference between the two is attributed to secondary dissociation of N_3. The solid vertical line indicates the energy of the barrier to dissociation for cyclic N_3. The dash-dotted vertical line shows the energy of the barrier to dissociation for linear N_3. The dashed vertical line shows the energy of the lowest cyclic N_3 doublet/quartet seam of crossing. The dotted vertical line shows the energy of the highest energy doublet/quartet surface seam of crossing for linear N_3.

Figure 3 shows the momentum matched N_3 photofragments observed when the QMF is adjusted to pass $m/z = 42$ (N_3^+). Due to its nearly three times higher mass, this TOF spectrum shows signal at arrival times substantially later than for CH_3^+, (earliest signal ~50 μs compared to 20 μs for CH_3). The solid lines passing through the data in Figures 2 and 3 are obtained from a forward convolution analysis using the program PHOTRAN. From this computational simulation of the experiment two COM translational energy release distributions, $P(E_T)$, are obtained for the C−N bond cleavage reaction producing CH_3 and N_3 from CH_3N_3. These two $P(E_T)$'s are shown in Figure 4. Here, the $P(E_T)$ derived from the $m/z = 15$ data is shown as open circles, whereas the $P(E_T)$ derived from the $m/z = 42$ data is shown as closed circles. One might at first wonder why we obtain different translational energy distributions for the C−N bond cleavage reaction depending on which photofragment we observe. However, when one realizes that the CH_3 fragment is energetically much more stable with respect to

unimolecular dissociation than the N_3 fragment, one will begin to understand this subtlety. Specifically, dissociation to produce $CH_2 + H + N_3$ would require about 35 kcal/mol additional energy than is available under the conditions of this work. This channel would only appear above an energy of 259 kcal/mol in Figure 1. In contrast, cyclic N_3 may dissociate through a spin-allowed channel if less than about 11 kcal/mol of translational energy appears and through a spin forbidden channel if less than about 18 kcal/mol of translational energy appear.[11,28] The vertical solid line in Figure 4 indicates the energy above which only the spin-forbidden dissociation (or perhaps tunneling through the spin allowed dissociation barrier) is possible. The vertical dashed line shows the maximum translational energy possible for the spin-forbidden dissociation channel. Assuming cyclic N_3 formation, if we assign the fraction of N_3 dissociation taking place at energies above the demarcation to the spin-forbidden channel (solid vertical line), by comparison of the integrated areas for spin forbidden vs spin allowed dissociation, we would conclude that the spin-allowed channel is more important by at least a factor of 4.5:1. Furthermore, analogous to the photodissociation of N_3 that has been previously reported at 248 nm[3], we cannot rule out that at least some of the N_3 produced in this work may absorb a second 193-nm photon, removing some of the N_3 reactive flux appearing at the mass spectrometric detector.

It is important to take note of the fact that the two $P(E_T)$'s in Figure 4 are in excellent agreement for those dissociation events that release more than ~20 kcal/mol of translational energy. This is strong evidence that CH_3 and N_3 are a momentum matched product pair and that quartet-seam crossings for linear N_3 located at lower internal (higher translational) energies, are unimportant. It should be noted that linear N_3 may dissociate through a spin-allowed channel if less than about 15 kcal/mol of translational energy appears as shown in Figure 4 by the dash-dotted line. Although this is not far from the point where the two $P(E_T)$'s deviate, no further evidence for linear N_3 was observed in either the detected secondary dissociation products or the ionization threshold shown below. There is also no indication of dissociation through the spin forbidden channel to form linear N_3, the energy for which is also shown in Figure 4 as a dotted line.

Finally, we note that a small portion of the N_3 flux persists below $E_T \sim 11$ kcal/mol (the barrier to dissociation for the spin allowed channel). We attribute this to the simultaneous excitation of methyl internal degrees of freedom that result in lower internal energy of the N_3 at these values of E_T. If the methyl fragment were always cold, we would expect to see an immediate drop to 0 below 11 kcal/mol in the $P_{42}(E_T)$. This deviation is representative of the methyl fragment's internal energy distribution which can be estimated by the difference between these two $P(E_T)$'s as follows: $P_{CH3}(E_{in}) \approx P_{15}(20\text{-}E_T) - P_{42}(20\text{-}E_T)$, which is shown in Figure 5. From this analysis, we can clearly see the approach to 0-CH_3 internal excitation; thus, we will also be able to see it in the analysis of the maximum translational energy release.

We have also obtained direct evidence for secondary dissociation of N_3, which is shown in Figure 6. In this experiment we have tuned the undulator gap to produce VUV ionizing radiation at $h\nu = 13.3$ eV. At this energy, photons are not capable of ionizing the N(^{4}S) or to dissociatively ionize $CH_3 \rightarrow CH_2^+ + H$. Only the spin-allowed dissociation product of N_3, N(^{2}D), can be ionized under these conditions. The closed circles in Figure 6 show the data re-binned to 2-μs channels. The solid line passing through the data is the result of the forward convolution analysis of secondary dissociation, which has been described previously.[3,4]

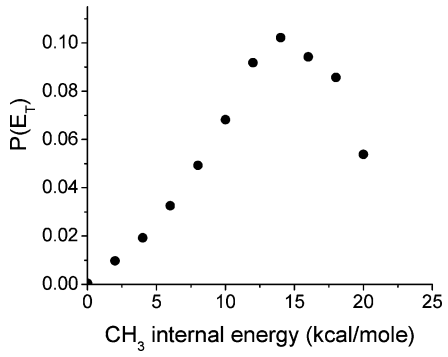

Figure 5. Estimated internal energy distribution of CH_3 fragment based on the differences in $P(E_T)$ for $m/z = 15$ and 42.

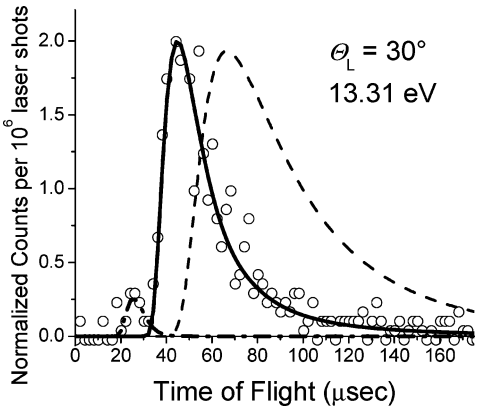

Figure 6. Observed TOF spectrum for $m/z = 14(N^+)$. The undulator was tuned to pass VUV ionizing radiation of 13.3 eV, sufficient only to ionize N(^{2}D). The data has been binned to 2 μs channels. The solid line fit to the data is the result of forward convolution analysis, using the program ANALMAX and gives rise the $P_{sec}(E_T)$ shown in Figure 6. The dashed curve shows the TOF predicted using a $P_{sec}(E_T)$ expected for the lower barrier of the linear dissociation channel. The dashed-dotted contribution shows a contribution attributed to some N(^{4}S) ionized by incomplete suppression of high-order undulator and/or white-light continuum radiation. The data has been normalized to laser power and the synchrotron radiation intensity.

In this fitting procedure, the difference $P(E_T)$, that is, the difference between the two $P(E_T)$'s shown in Figure 4, is used to characterize the translational motion of the N_3 molecules that undergo secondary dissociation. A second $P_{sec}(E_T)$ is derived from the best fit to the $m/z = 14$ TOF spectrum (solid line of Figure 6), which describes the translational energy release of the $N_3 \rightarrow N_2 + N(^2D)$ reaction, shown in Figure 7. Also shown in Figure 6 is forward convolution simulated TOF for a hypothetical $P(E_T)$ peaking at 2 kcal/mol, similar to what would be expected for secondary dissociation of linear N_3, which takes place over a 3-kcal/mol exit barrier.[28] This model is clearly inconsistent with observation.

We also found a weak channel in the $m/z = 14$ TOF (fit by the dashed-dotted line) shown in Figure 6, which exhibits a much larger translational energy release, and we ascribe this channel to a small amount of N(^{4}S) from the spin forbidden dissociation being ionized by the higher order harmonics of the synchrotron radiation which makes it through the buffer gas. Due to the very small intensity, even under significant binning, it is difficult to perform precise quantitative analysis on this peak. The secondary fitting seen in Figure 6 has a maximum translational energy release at 42 kcal/mol which can be

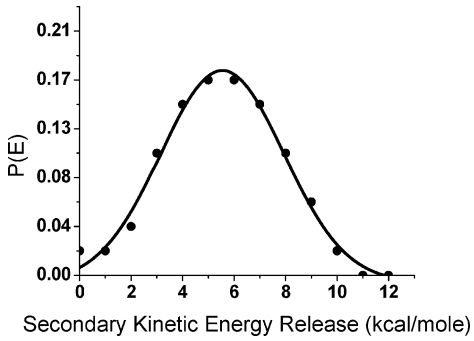

Figure 7. Translational energy release obtained from analysis from the $m/z = 14$ data of Figure 5, describing the translation energy release of the reaction $N_3 \rightarrow N_2 + N(^2D)$. A Gaussian has been fitted to the points for clarity.

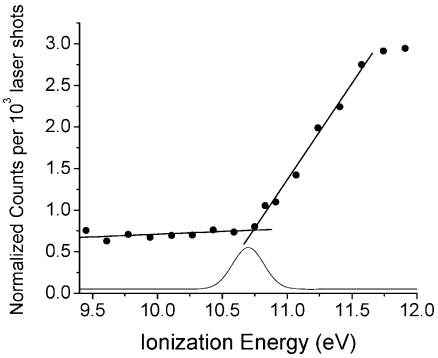

Figure 8. Ionization energy dependence of the $m/z = 42$ TOF signal. The bandwidth function of the undulator is shown as a Gaussian. The data was integrated over the arrival time and has been normalized to laser power and the synchrotron radiation intensity.

consistent with $N(^4S)$. In addition, the relative magnitude of this peak increases in data acquired with ionization energy of 15.9 eV. However, CH_2^+ from dissociative ionization of CH_3 fragments starts to obscure this data, so a detailed quantitative analysis of the peak we attribute to $N(^4S)$ is still not possible.

In another set of experiments similar to a recently reported study,[13] we examined the dependence of the $m/z = 42$ signal on the undulator gap, which is used to vary the wavelength of the ionizing synchrotron radiation. Figure 8 shows the TOF-integrated ($m/z = 42$) signal at a laboratory angle of $\Theta_L = 60°$ vs the energy of the ionizing photons. The signal has been carefully normalized to the laser power, number of laser shots, and the synchrotron radiation's intensity. The background seen at low photoionization energies results from the "white light continuum" produced by the undulator. The intersection of the two straight lines provides an accurate estimate of the ionization potential of the N_3 formed in this experiment We derive from this that the N_3 formed in this work exhibits an ionization threshold (IP) of 10.7 eV, consistent with previous experimental and theoretical results for cyclic N_3.

B. N−N Bond Rupture "Molecular" Channel. We have previously reported a collision free photochemical dissociation mechanism for methyl azide at 248 nm,[10] which is summarized below.

Initiation

$H_3C-N-N\equiv N \rightarrow H_3C-N + N_2$ (R1, molecular elimination)

$H_3C-N + N_2 \rightarrow H_2C=NH + N_2$ (isomerization)

HCN Formation

$H_2C=NH \rightarrow H_2C=N + H$ (R4, simple bond rupture)

$H_2C=N \rightarrow HC\equiv N + H$ (R6, simple bond rupture)

HNC Formation

$H_2C=N-H \rightarrow H_2 + C\equiv NH$ (R5, 1, 1 H_2 elimination)

In the present experiments at 193 nm, we recorded TOF spectra at m/z values of 27, 28, and 29 in an effort to detect similar photochemistry. Figure 9 shows a series of TOF spectra (data as open circles) and forward convolution fitting (shown as lines) for the m/z values related to this dissociation pathway (m/z = 27, 28, and 29). The results are similar to what we reported at 248 nm;[10] however, there are some difference which make the interpretation of this data less definitive.

The top panel of Figure 9 shows a representative TOF spectrum for $m/z = 29$ (CH_2NH^+). The corresponding $P(E_T)$ used to fit this data is shown in Figure 10 as solid circles. As seen in previous work, only a small fraction of the available energy goes into translation of the $m/z = 29$ fragment. Assuming direct methanimine formation (referred to as R3 in our previous work) approximately 200 kcal/mol of energy is available. Assuming reaction R1 (singlet methyl-nitrene) only 110 kcal/mol of energy is available. The average energy release observed in this work is only ~35 kcal/mol, 31.5% of the energy available to R1 or 17% of the energy available to R3. We previously rationalized similar observations at 248 nm pointing out that it would be unusual to form two closed shell products ($CH_2NH + N_2$) with such low (17%) translational energy release. Using the soft product impulse approximation,[30] we previously found the COM translational energy release for R1 to be closer to expectations. In this work, the translational energy release for R1 from the soft product impulse approximation would be ~54 kcal/mol, whereas R3 would be ~100 kcal/mol. Following the same reasoning of our previous work, we conclude that reaction R1 is a more reasonable explanation of the observations.

The middle panel of Figure 9 shows a representative TOF spectra for $m/z = 28$. It should be noted the ionizing synchrotron radiation was not high enough to ionize N_2, which is the expected momentum matched product of reaction R1. Consequently, this spectrum is assigned to CH_2N, the result of H-atom loss from methanimine (CH_2NH). The fitting to the middle panel of Figure 9 was done with ANALMAX in a secondary dissociation product calculation. The resulting fit was obtained with a maximum energy release for the secondary channel of less than 1 kcal/mol, consistent with a barrier-less simple bond rupture mechanism.

The bottom panel of Figure 9 shows a representative TOF spectra for $m/z = 27$. Contrary to our previous work, where we were able to distinguish between the two reaction channels producing HCN and HNC, here there is little to no change in shape of the TOF spectrum as the photoionization is varied above and below the ionization threshold of HCN. In fact, the TOF spectrum peak is still clearly seen, albeit much weaker, at an ionization energy of 11.91 eV, below the IP for both HCN and HNC. This implies that, with the larger amount of internal energy available at 193 nm versus 248 nm, some highly excited HCN or HNC (indeed the vibrational wavefunctions may be delocalized over both wells[31−35]) are still detectable even at these photoionization energies. However, the spectra observed could be fit with ANALMAX with a secondary energy release of around 1 kcal/mol. Although this is technically a tertiary process, if we assume essentially zero kinetic energy release on the

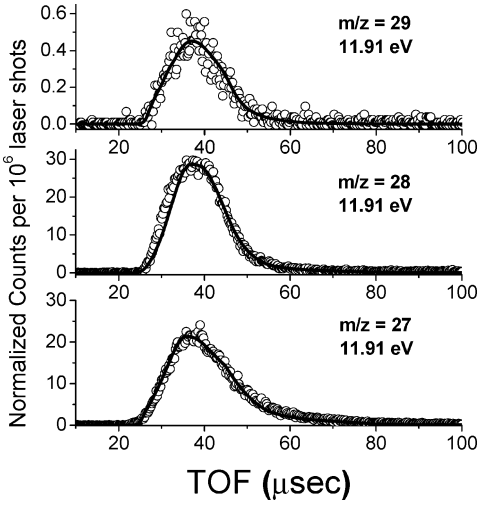

Figure 9. TOF spectra summarizing the results of the measurements on the N−N bond rupture channel. The open circle points are the observed data and the solid line is the result of forward convolution fitting from PHOTRAN and ANALMAX. All data was collected at $\Theta_L = 30°$ and a photoionization energy of 11.91 eV. The data has been normalized to laser power and the synchrotron radiation intensity.

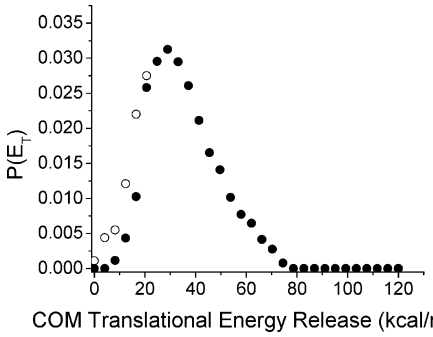

Figure 10. COM translation energy release diagram for the $CH_3N + N_2$ reaction channel. The solid circles fit the observed primary channel. The open circles are needed to fit the observed secondary channels.

secondary step, we can treat this reaction as a secondary dissociation. This assumption should be valid as the secondary release was shown to peak at less than 1 kcal/mol. This low-energy release is again consistent with simple bond rupture of an H atom and implies that the dominate channel at 193 nm is sequential loss of two H-atoms producing HCN. This is also consistent with the observation that we observe a large jump in intensity when we increase the ionizing photons over the IP of HCN.

It should also be noted that in order to obtain the best fit to the CH_2N^+ and HCN/HNC TOF spectrum (specifically to the slow tail), we could not use the primary $P(E_T)$ shown solid circles in Figure 10. Rather, it was necessary to use the $P(E_T)$ shown with open circles. We attribute this to a weak energy dependent dissociation probability for CH_2NH.

It is worth noting that the $m/z = 29{:}28$ intensity ratio is close the isotopic abundance expected for CH_2N^+. This would require (not unreasonably) that primary CH_3N product completely decomposes on the time scale of this experiment ($\sim 10^{-4}$ s). Nevertheless, detected signals at $m/z = 27$ must still be attributed to HCN/HNC and serve as unambiguous evidence for reaction (R1). The fact that the shape of the TOF distribution does not change dramatically across the 27/28/29 spectra is consistent with a low kinetic energy release in the secondary dissociation steps, suggesting that HCN, which is formed by sequential N−H and C−H bond rupture may dominate over HNC, which is formed by H_2 elimination.

C. Estimate of the Branching Ratio. It is a logical question to inquire about the branching ratio between C−N and N−N bond rupture. Unfortunately, given the lack of knowledge of relative photoionization cross-sections for all of the observed products, some of which are highly internally excited, it would be misleading to report any numerical quantity. What we can report is that both channels are easily observed in this work, and we therefore tend to surmise that neither channel dominates the dissociation. However, a naive analysis assuming equal ionization probabilities for N_3, CH_2NH, CH_2N, and HCN/HNC would lead us to conclude that N−N bond cleavage is the more important channel, but this should be taken with an appropriate shovel full of salt grains. Experiments like the ones presented here, but employing electron impact ionization could answer this important question accurately, as electron impact ionization cross-sections can be estimated reasonably accurately.

Conclusions

Photolysis of methyl azide at 193 nm has been carried out and the C−N bond rupture channel producing N_3 from methyl azide photolysis has been observed. From the forward convolution fitting of the TOF spectra for $m/z = 42$, we obtain a maximum COM translational energy release for the $N_3 + CH_3$ channel of $E_T^{max} = 45 \pm 4$ kcal/mol. This is close to the expected energy limit for cyclic N_3 predicted from literature heats of formation. In contrast, if linear N_3 were formed, there would be approximately 30 kcal/mol of excess energy unaccounted for. The characteristics of the translational energy distribution for the secondary dissociation of N_3 also support the conclusion of exclusive cyclic N_3 production. The maximum COM translational energy release for the secondary dissociation producing $N(^2D)$ and N_2 that we derived from the $m/z = 14$ TOF spectra is 11 kcal/mol and the distribution peaks at ~6 kcal/mol. This is in good agreement with the theoretically predicted exit channel barrier (7 kcal/mol) for cyclic N_3 dissociation to form $N_2 + N(^2D)$ and substantially higher than the theoretically predicted exit channel barrier (3 kcal/mol) for linear N_3 dissociation. The N_3 ionization threshold found in this work (10.7 eV) closely mirrors that obtained in previous work on ClN_3 photolysis where cyclic N_3 was also present (10.67 eV) and agrees with theoretical predictions for the cyclic structure. All of the available evidence strongly suggests exclusive production of cyclic N_3. Furthermore, we observe that about 45% of the N_3 product does not dissociate on the 10^{-4} s time scale. A key remaining unanswered question is the branching ratio between the N−N bond rupture channel and the C−N bond rupture channel.

Acknowledgment. This work was in part supported by a grant from the Air Force Office of Scientific Research (Grant. No. FA9550-07-1-0206). We thank Institute of Atomic and Molecular Sciences, Academia Sinica, Taipei, Taiwan for financial support and the National Synchrotron Radiation Research Center personnel for their help in conducting those experiments. We also thank Jeff Bode and Alex Lippert for their assistance in synthesizing our methyl azide sample.

References and Notes

(1) Samartzis, P. C.; Wodtke, A. M. *Int. Rev. Phys. Chem.* **2006**, *25*, 527.

(2) Samartzis, P. C.; Wodtke, A. M. *Phys. Chem. Chem. Phys.* **2007**, *9*, 3054.

(3) Hansen, N.; Wodtke, A. M.; Goncher, S. J.; Robinson, J. C.; Sveum, N. E.; Neumark, D. M. *J. Chem. Phys.* **2005**, *123*.
(4) Wodtke, A. M.; Hansen, N.; Robinson, J. C.; Sveum, N. E.; Goncher, S. J.; Neumark, D. M. *Chem. Phys. Lett.* **2004**, *391*, 334.
(5) Samartzis, P. C.; Hansen, N.; Wodtke, A. M. *Phys. Chem. Chem. Phys.* **2006**, *8*, 2958.
(6) Hansen, N.; Wodtke, A. M. *J. Phys. Chem. A* **2003**, *107*, 10608.
(7) Hansen, N.; Wodtke, A. M.; Komissarov, A. V.; Morokuma, K.; Heaven, M. C. *J. Chem. Phys.* **2003**, *118*, 10485.
(8) Hansen, N.; Wodtke, A. M.; Komissarov, A. V.; Heaven, M. C. *Chem. Phys. Lett.* **2003**, *368*, 568.
(9) Goncher, S. J.; Sveum, N. E.; Moore, D. T.; Bartlett, N. D.; Neumark, D. M. *J. Chem. Phys.* **2006**, *125*.
(10) Larson, C.; Ji, Y. Y.; Samartzis, P.; Wodtke, A. M.; Lee, S. H.; Lin, J. J. M.; Chaudhuri, C.; Ching, T. T. *J. Chem. Phys.* **2006**, *125*.
(11) Zhang, J. Y.; Zhang, P.; Chen, Y.; Yuan, K. J.; Harich, S. A.; Wang, X. Y.; Wang, Z.; Yang, X. M.; Morokuma, K.; Wodtke, A. M. *Phys. Chem. Chem. Phys.* **2006**, *8*, 1690.
(12) Samartzis, P. C.; Lin, J. J. M.; Ching, T. T.; Chaudhuri, C.; Lee, S. H.; Wodtke, A. M. *J. Chem. Phys.* **2007**, *126*, 041101.
(13) Samartzis, P. C.; Lin, J. J. M.; Ching, T. T.; Chaudhuri, C.; Lee, Y. T.; Lee, S. H.; Wodtke, A. M. *J. Chem. Phys.* **2005**, *123*.
(14) Quinto-Hernandez, A.; Lee, Y.-Y.; Huang, T.-P.; Pan, W.-C.; Lin, J. J.-M.; Bobadova-Parvanova, P.; Morokuma, K.; Samartzis, P. C.; Wodtke, A. M. *Int. J. Mass Spectrom.* **2007**, *265*, 261.
(15) Patel, D.; Pritt, A. T.; Benard, D. J. *J. Phys. Chem.* **1986**, *90*, 1931.
(16) Getoff, N.; Laupert, R.; Schindle. Rn. *Z. Phys. Chem.-Frankfurt* **1970**, *70*, 70.
(17) Babikov, D.; Mozhayskiy, V. A.; Krylov, A. I. *J. Chem. Phys.* **2006**, *125*.
(18) Tarroni, R.; Tosi, P. *Chem. Phys. Lett.* **2004**, *389*, 274.
(19) Lin, J. J.; Chen, Y.; Lee, Y. Y.; Lee, Y. T.; Yang, X. M. *Chem. Phys. Lett.* **2002**, *361*, 374.
(20) Bock, H.; Dammel, R. *Angew. Chem., Int. Ed.* **1987**, *26*, 504.
(21) Hassner, A.; Stern, M.; Gottlieb, H. E.; Frolow, F. *J. Org. Chem.* **1990**, *55*, 2304.
(22) Harich, S. A. PHOTRAN: A program for forward convolution analysis of photodissociation, 2003.
(23) Wodtke, A. M. Very High Resolution Photofragmentation-Translational FSpectroscopy. Ph.D. Thesis; University of California: Berkeley, CA, 1986.
(24) Gutowski, K. E.; Rogers, R. D.; Dixon, D. A. *J. Phys. Chem. A* **2006**, *110*, 11890.
(25) Ruscic, B.; Boggs, J. E.; Burcat, A.; Csaszar, A. G.; Demaison, J.; Janoschek, R.; Martin, J. M. L.; Morton, M. L.; Rossi, M. J.; Stanton, J. F.; Szalay, P. G.; Westmoreland, P. R.; Zabel, F.; Berces, T. *J. Phys. Chem. Ref. Data* **2005**, *34*, 573.
(26) Continetti, R. E.; Cyr, D. R.; Metz, R. B.; Neumark, D. M. *Chem. Phys. Lett.* **1991**, *182*, 406.
(27) Continetti, R. E.; Cyr, D. R.; Osborn, D. L.; Leahy, D. J.; Neumark, D. M. *J. Chem. Phys.* **1993**, *99*, 2616.
(28) Zhang, P.; Morokuma, K.; Wodtke, A. M. *J. Chem. Phys.* **2005**, *122*.
(29) Continetti, R. E.; Balko, B. A.; Lee, Y. T. *J. Chem. Phys.* **1988**, *89*, 3383.
(30) Riley, S. J.; Wilson, K. R. *Faraday Discuss.* **1972**, 132.
(31) Barger, T.; Wodtke, A. M.; Bowman, J. M. *Astrophys. J.* **2003**, *587*, 841.
(32) Bowman, J. M.; Irle, S.; Morokuma, K.; Wodtke, A. *J. Chem. Phys.* **2001**, *114*, 7923.
(33) Jonas, D. M.; Yang, X. M.; Wodtke, A. M. *J. Chem. Phys.* **1992**, *97*, 2284.
(34) Yang, X. M.; Wodtke, A. M. *J. Chem. Phys.* **1990**, *93*, 3723.
(35) Yang, X. M.; Rogaski, C. A.; Wodtke, A. M. *J. Chem. Phys.* **1990**, *92*, 2111.